Heliyon 10 (2024) e38918

Contents lists available at ScienceDirect

Heliyon

journal homepage: www.cell.com/heliyon

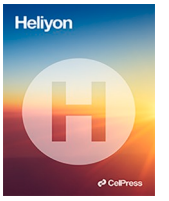

Research article

NUPR1 modulates pulmonary embolism progression via smooth muscle cells phenotypic transformation

Shu Wang [a], Aizhen Xu [a], Maoqing Chen [a], Yue Wu [b,*]

[a] Department of Respiratory and Critical Care Medicine, Zibo Central Hospital, Zibo, Shandong, 255036, China
[b] Department of Vascular Surgery, Zibo Central Hospital, Zibo, Shandong, 255036, China

ARTICLE INFO

Keywords:
Pulmonary embolism
Pulmonary artery smooth muscle cells
NUPR1
Phenotypic shift
Glycolysis

ABSTRACT

Objective: This study aimed to investigate the role of Nuclear Protein 1 (NUPR1) in pulmonary embolism (PE) and its impact on the phenotypic transformation of pulmonary artery smooth muscle cells (PASMCs).

Methods: A PE model was established via autologous pulmonary emboli infusion into the jugular vein. Partial Pressure of Oxygen (PaO2), Oxygenation Index (OI), Brain Natriuretic Peptide (BNP), and Troponin I (TnI) were measured, and lung tissue was subjected to hematoxylin-eosin (HE) staining. NUPR1 expression was assessed through Immunofluorescence and Western blot analyses. To investigate role of NUPR1, PE rats were treated with lentiviral vectors for NUPR1 knockdown (si-NUPR1) or overexpression (ov-NUPR1), and the effects on lung pathology were examined. NUPR1 expression was evaluated in human PASMCs. Additionally, PASMCs from SD rats were cultured under normoxic and hypoxic conditions to evaluate NUPR1 expression. Transfection of NUPR1 expression vectors into PASMCs allowed monitoring of phenotypic transformation-associated protein changes and PASMCs activity.

Results: Increased NURP1 was observed in human-derived PASMCs. In PE rats, histological examination revealed ruptured pulmonary alveoli, exudate accumulation, interstitial edema, and infiltration of inflammatory cells, concomitant with elevated NUPR1 expression levels. Knockdown of NUPR1 in PE rats significantly improved lung tissue structure, reducing alveolar rupture and interstitial edema. Conversely, NUPR1 overexpression exacerbated lung damage, leading to increased inflammatory infiltration. NUPR1 expression in rat PASMCs remained stable under normoxic conditions; however, under hypoxic conditions, NUPR1 protein expression increased progressively over time. Subsequent upregulation of NUPR1 expression led to a decrease in the levels of contractile phenotype markers α-SMA and SM22α in PASMCs, accompanied by increased expression of synthetic phenotype markers Vimentin and OPN. This phenotypic shift was associated with enhanced cellular proliferation, invasion, and migration.

Conclusions: Elevated NUPR1 expression in PE exacerbates abnormal PASMCs proliferation by promoting their phenotypic transformation, thereby fostering the pathological progression of PE.

1. Introduction

Pulmonary embolism (PE) is a clinicopathophysiological syndrome characterized by the blockage of pulmonary arteries and their

* Corresponding author.
E-mail address: wuyue-0202@163.com (Y. Wu).

https://doi.org/10.1016/j.heliyon.2024.e38918
Received 25 May 2024; Received in revised form 1 October 2024; Accepted 2 October 2024
Available online 3 October 2024

branches due to emboli detaching from the systemic circulation [1]. PE is a significant health concern in the United States, resulting in approximately 100,000 deaths annually, with 30-day and 1-year mortality rates of about 4 % and 13 %, respectively [2,3]. Common clinical manifestations include dyspnea, hemoptysis, and chest pain, which can be life-threatening in severe cases [4]. PE is frequently associated with deep vein thrombosis, a combination known as venous thromboembolism [5]. Additionally, PE underlies various conditions such as tuberculosis, chronic obstructive pulmonary disease, and pulmonary hypertension, posing significant health risks [6]. Therefore, A thorough understanding of PE pathogenesis is crucial for developing new diagnostic and therapeutic strategies [7].

The initial treatment of PE focused on anticoagulation and systemic thrombolytic therapy for life-threatening cases [8]. This approach aims to prevent further clot formation and promote natural thrombus dissolution. In the context of PE-induced pulmonary vascular remodeling, pathological changes such as the over-proliferation, migration, resistance to apoptosis, and phenotypic transformation of pulmonary artery smooth muscle cells (PASMCs) play critical roles [9]. Targeting these pathological behaviors may offer new therapeutic directions for PE [10].

Nuclear protein 1 (NUPR1) is a multifunctional nucleoprotein involved in stress regulation and has been shown to be essential in various diseases [11–13]. This stress-response gene is upregulated by numerous biological and chemical stressors such as TNFα, lipopolysaccharides, amino acid deprivation, and cannabinoids [14,15,50,16]. Recent research highlights NUPR1's significance in the growth of multiple human malignant tumor cells (Shan Liu & Max Costa, 2022; [17]). Beyond cancer, NUPR1 influences various cellular life cycle changes and stimulates physiological behaviors such as ferroptosis and autophagy [18]. For instance, knockdown of NUPR1 enhances the sensitivity of non-small-cell lung cancer cells to metformin by inhibiting the AKT pathway [19] and its knockdown inhibits angiogenesis in lung cancer through the IRE1/XBP1 and PERK/eIF2α/ATF4 signaling pathways [20]. Additionally, NUPR1 mediates PASMCs phenotypic transformation via the STIM1 signaling axis, which induces pulmonary arterial hypertension [21]. NUPR1 also induces smooth muscle cell fibrosis in the lungs and promotes epithelial-mesenchymal transition [22]. These findings imply that NUPR1 may play a crucial role in regulating PASMCs. However, its role in PE remains underexplored, and investigating this could reveal NUPR1 as a key diagnostic and therapeutic target for PE.

Based on these insights, we hypothesize that NUPR1 significantly affects the secretion and phenotypic transformation of PASMCs (pulmonary artery smooth muscle cells) and is intricately involved in the progression of PE. By elucidating the role of NUPR1 in PE, we aim to provide new insights and guidance for the clinical diagnosis and treatment of this condition.

2. Materials and methods

2.1. Animal data

We purchased 70 specific pathogen-free (SPF) Sprague-Dawley (SD) rats, aged 8–10 weeks and weighing (280 ± 10) grams, from Nantong Jingqi Biotech Co., Ltd. (Animal Use License No. SYXK (Su) 2023-0028). The rats were housed in a controlled environment with a 12-h light/dark cycle at a temperature of 24 °C, with ad libitum access to food and water. After one week of acclimatization, pulmonary embolism (PE) modeling was performed. This study was approved by the Animal Ethics Committee of our hospital (No. 2023WSA010008) and was conducted in strict accordance with the principles of the 3Rs: "Reduce, Refine, and Replace".

2.2. Establishment of animal model

Fifty rats were randomly selected for PE modeling by infusion of autologous pulmonary emboli via intravenous jugular vein infusion (Y. [23]). To create the emboli; 0.5 mL of blood was collected from the orbital vein of each rat. After coagulation, the clot was divided into approximately 20 thrombus emboli, each measuring 0.5 × 2 mm^2. These emboli were then placed into a 2 mL sterile syringe and mixed with normal saline to form a thrombus suspension.

The rats were anesthetized with an intraperitoneal injection of sodium pentobarbital at a dose of 50 mg/kg. A longitudinal incision of approximately 1 cm was made on the right side of the neck to expose the jugular vein. The thrombus suspension (containing about 20 emboli) was then quickly injected into the right common jugular vein. Following the injection, the incision site was disinfected and sutured. The successful establishment of the PE model was confirmed when the rats exhibited cyanosis and gradually accelerated and deepened breathing within 2 h post-operation. Another twenty rats were used as a control group and were fed normally without any intervention. Ten PE rats (labeled as model group) and ten control rats were randomly selected. After anesthesia, the abdominal cavity of the rat was opened to expose the abdominal aorta and blood were collected using an ordinary negative pressure tube for serum separation to measure brain natriuretic peptide (BNP) and troponin I (TnI) levels. Additionally, another 2 mL of blood was drawn from the abdominal aorta using an anticoagulant negative pressure tube to determine the arterial partial pressure of oxygen (PaO2) with a blood gas analyzer and to calculate the oxygenation index (OI). Following these procedures, the rats were euthanized using isoflurane. Lung tissues were then collected for histological examination. The remaining ten rats were used to culture PASMCs as described in section 2.9.

2.3. Enzyme-linked immunosorbent assay (ELISA)

ELISA was used to measure BNP and TnI levels in the serum of mice. Briefly, following sample preparation, including the collection and centrifugation of blood from the abdominal aorta, ELISA plates were coated with specific capture antibodies for BNP and TnI. After blocking to prevent non-specific binding, serum samples along with standards were added to the wells and allowed to incubate. Subsequent steps involved the addition of biotinylated detection antibodies, streptavidin-conjugated horseradish peroxidase (HRP),

and TMB substrate solution. The resulting color development was measured spectrophotometrically at 450 nm. By comparing optical density (OD) values to a standard curve, we quantified the concentration of BNP and TnI in the serum samples and presented as bar graphs.

2.4. Hematoxylin and eosin staining

The rats were euthanized, and lung tissue from different groups was collected and fixed in 10 % formaldehyde for 24 h. The tissues were then transferred to 70 % ethanol for dehydration, followed by waxing and embedding in paraffin to prepare paraffin blocks. The embedded tissues were sliced into 4–6 μm sections to prepare slides for hematoxylin-eosin (H&E) staining. Briefly, The slides were deparaffinized in xylene to remove the paraffin wax. They were then rehydrated by passing them through a series of graded alcohol solutions, decreasing in concentration, followed by rehydration in water. Next, the slides were stained with hematoxylin to highlight the cell nuclei and eosin to stain the cytoplasm and other tissue components. Following staining, the tissue slides were rinsed with tap water for 5 min to eliminate excess dye. Mounting media was then applied on top of the tissue sections, which were covered with cover slips. The slides were placed under a hood for 24 h to allow the mounting media to dry. After drying, the slides were sealed with mounting media to preserve the stained sections and prepare them for microscopic (Olympus) examination.

2.5. Western blot

Total protein was extracted from human PASMCs and homogenized lung tissues, and the protein content was quantified using the BCA kit (Beyotime, Shanghai, China). Proteins were separated on a 12 % SDS-PAGE gel and transferred to a PVDF membrane, which was blocked with 5 % non-fat dry milk for 1 h. The membranes were then incubated overnight with primary antibodies, including Osteopontin (OPN) (Abcam #ab8448, 1:1000), SM22α/Transgelin (Cell Signaling Technology #52011, 1:400), α-SMA (Cell Signaling Technology #19245, 1:500), Vimentin (Santa Cruz #32322, 1:50), GLUT1 (Proteintech #21829-1-AP, 1:350), Pyruvate Dehydrogenase Kinase 1/PDK1 (Proteintech #18262-1-AP, 1:500), Lactate Dehydrogenase/LDHA (Cell Signaling Technology #2012, 1:800), Monocarboxylate Transporter 4/MCT4 (Santa Cruz #376140, 1:50), and Pyruvate Dehydrogenase/PDH (Cell Signaling Technology #2784, 1:600), Ki-67 (Abcam #ab197547, 1:1000), PCNA (Abcam #ab92552, 1:1000), Bax (Abcam #ab32503, 1:1000), Bcl-2 (Abcam #ab182858, 1:1000). The next day, the membranes were incubated with secondary antibodies (anti-mouse, Abcam #67281, 1:1000, and anti-rabbit, Abcam #ab6721, 1:900) for 2 h at room temperature. After washing four times with TBST solution, an ECL developer was added dropwise to detect the protein bands. The uncropped western blots have been provided as a supplementary figure.

2.6. Immunofluorescence

The lung tissue slides were deparaffinized in xylene, rehydrated in graded alcohol series, and then in water. Following this, the slides were treated with blocking buffer (BSA)+0.3 % Triton-PBS at room temperature for 20 min to permeabilize the tissues and block nonspecific binding sites. After blocking, the slides were incubated overnight at 4 °C with a primary antibody against NUPR1 (Proteintech# 15056-1-AP, 1:300). The next day, the slides were washed with PBS and incubated for 1 h at room temperature with an anti-rabbit secondary antibody (Thermofisher#A-11008 1:500) in the dark. Subsequently, the nuclei were stained with DAPI for 10 min. Finally, the stained tissue sections were observed and photographed using a laser confocal microscope.

2.7. NUPR1 modulation and its effects on PE rats

Thirty PE rats were randomly assigned to three experimental groups (n = 10 per group). The groups included: (1) a NUPR1 knockdown group, which received a lentiviral vector for NUPR1 interference (si-NUPR1), (2) a NUPR1 overexpression group, which received a lentiviral vector to elevate NUPR1 expression (ov-NUPR1), and (3) a control group, which received a NUPR1 empty vector (nc-NUPR1). All lentiviral vectors were synthesized by Guangzhou Sayer Biologicals, with a viral titer of 1×10^8 PFU/mL. Each group was administered 100 μL of the respective lentiviral vector via tail vein injection prior to PE induction. Additionally, a control group of 10 healthy rats received an equal volume (100 μL) of saline injected via the tail vein. Following the completion of the PE modeling procedure, lung tissue samples were collected from all groups, and histological analysis was performed using H&E staining, as outlined in section 2.4.

2.8. Clinical data

Twenty patients with PE admitted to our hospital between April 2023 and January 2024 were included in this study. Inclusion criteria required a confirmed PE diagnosis through imaging, suitability for pulmonary artery thrombectomy, and surgery performed by the same surgical team at our hospital. Patients with other lung diseases or respiratory conditions were excluded. Proliferative endothelial tissues resected during surgery were collected for PASMC culture, serving as the research group. Additionally, human PASMCs from Bei Na Biotechnology Co., Ltd. were used as a control/normal group. The PASMCs were cultured in DMEM/F12 complete medium with 10 % FBS and 1 % PS. This study was ethically approved by the Zibo hospital's Ethics Committee, and all participants provided informed consent (No. 20230108).

2.9. Primary PASMCs culture

For the primary PASMCs culture, SD rats were humanely euthanized by cervical dislocation under anesthesia induced by pentobarbital sodium (2 %), followed by immersion in 75 % alcohol for 5 min to ensure sterility. The intact lung tissue was carefully excised and meticulously dissected along the main pulmonary artery, meticulously removing the surrounding connective tissue under a microscope (the proliferating endothelial tissue of PE patients was also treated in this way). Subsequently, the blood vessels were longitudinally incised, and the tunica intima was delicately removed using a sterile surgical blade, while the tunica externa was separated under a stereomicroscope. The isolated tunica media tissue was then finely minced and enzymatically digested in a 0.2 % collagenase II solution at 37 °C for 30 min. Following digestion, the solution was centrifuged at 800 revolutions per minute (rpm) for 5 min to discard the supernatant. The resulting cell precipitates were resuspended in 5 mL of Dulbecco's Modified Eagle Medium/Nutrient Mixture F-12 (DMEM/F12) supplemented with 20 % fetal bovine serum (FBS) and 1 % penicillin-streptomycin (PS). Upon filling the culture flask, the cells underwent purification through three rounds of differential attachment. Subsequently, starting from the second generation, PASMCs were maintained in a DMEM/F12 complete medium supplemented with 10 % FBS and 1 % PS.

2.10. Hypoxic treatment of PASMCs

During the logarithmic growth phase, 5×10^4 PASMCs were seeded into a 25 cm^2 cell culture flask for cultivation. The cells were then exposed to hypoxic conditions (1 % O_2) for varying durations: 0, 6, 12, and 24 h. At each time point, the cells were harvested for analysis of NUPR1 protein expression. Concurrently, control cells were maintained under standard culture conditions (normoxia) and collected at corresponding time intervals for NUPR1 detection, employing the same analytical approach. This experimental setup facilitated the examination of NUPR1 expression under both hypoxic and normoxic conditions, providing insights into the cellular response to varying oxygen levels.

2.11. Seahorse experiment

The Seahorse experiment involved detaching adherent cells by digesting them with 0.25 % trypsin, followed by centrifugation at 1000 rpm for 5 min. The cells were then resuspended in serum-containing medium at a concentration of 1×10^5 cells/mL. the XF 24 cell culture plate was prepared aseptically, with background-corrected wells in positions A1, B4, C3, and D6. A total of 100 μL of cell growth medium was added to each well, followed by the inoculation of 100 μL of the cell suspension. After allowing the cells to settle for 1 h, mitochondrial basal and maximal respiration were assessed using the Seahorse XFe 24 instrument from Agilent, USA. The assay results were subsequently reviewed, and the data were normalized.

2.12. Transfection of NUPR1 lentiviral vectors

PASMCs were seeded into 24-well plates at a density of 10,000 cells per well and allowed to adhere overnight under standard culture conditions. Subsequently, cells were subjected to hypoxic conditions (1%O2) for 48 h prior to transfection. PASMCs were transfected using lentiviral vectors targeting NUPR1 interference expression (si-NUPR1), upregulated expression (ov-NUPR1), and negative control sequence (nc-NUPR1). Transfection of the lentiviral vectors into PASMCs was performed using Lipofectamine 3000 in Opti-MEM medium according to the manufacturer's protocol. After transfection, cells were maintained under both hypoxic and normoxic conditions for an additional 48 h. Verification of successful transfection was carried out by assessing proteins level of NUPR1.

2.13. Edu and Ki67 staining for PASMCs activity detection

Following the inoculation of PASMCs into a 24-well plate, 100 μL of preheated EdU solution (abcam#647, 10 μmol/L) was added for a 2-h incubation period in accordance with the manufacturer's instructions. Subsequently, PASMCs underwent immobilization with 4 % paraformaldehyde for 30 min, followed by the addition of 100 μL of Click reaction solution after washing, and a further 1-h incubation at room temperature shielded from light. Nuclear staining was then conducted by adding 100 μL of 1 × Hoechst 33342 per well. Fluorescence microscopy was employed to capture images, and the ratio of EdU-positive cells to Hoechst 33342-positive cells was calculated.

For the detection of Ki67-positive cells, cultured cells were treated with 0.3–0.5 % Triton X-100 for 15 min, followed by washing with PBS for 3 min and subsequent serum blocking at room temperature for 30 min. A Ki-67 antibody (Cell Signaling Technology#9129, 1:1000) was applied and incubated overnight in a humidified chamber at 4 °C, followed by a 1-h incubation with a secondary antibody (ThermoFisher, Alexa Fluor# A-11008, 1:2000) at room temperature in the dark. Following PBS washing, nuclei were stained with DAPI for 10 min. The cells were then mounted on slides and covered with cover slips prior to imaging using a fluorescence microscope.

2.14. Transwell and scratch-wound assay

For the Transwell assay, PASMCs were seeded into the upper compartment of transwell inserts with 8 μm pores, which were subsequently placed in a 24-well plate containing serum-free medium. After incubation, non-migrating cells on the inner membrane of the upper compartment were carefully removed, while the outer membrane containing migrating cells was fixed with

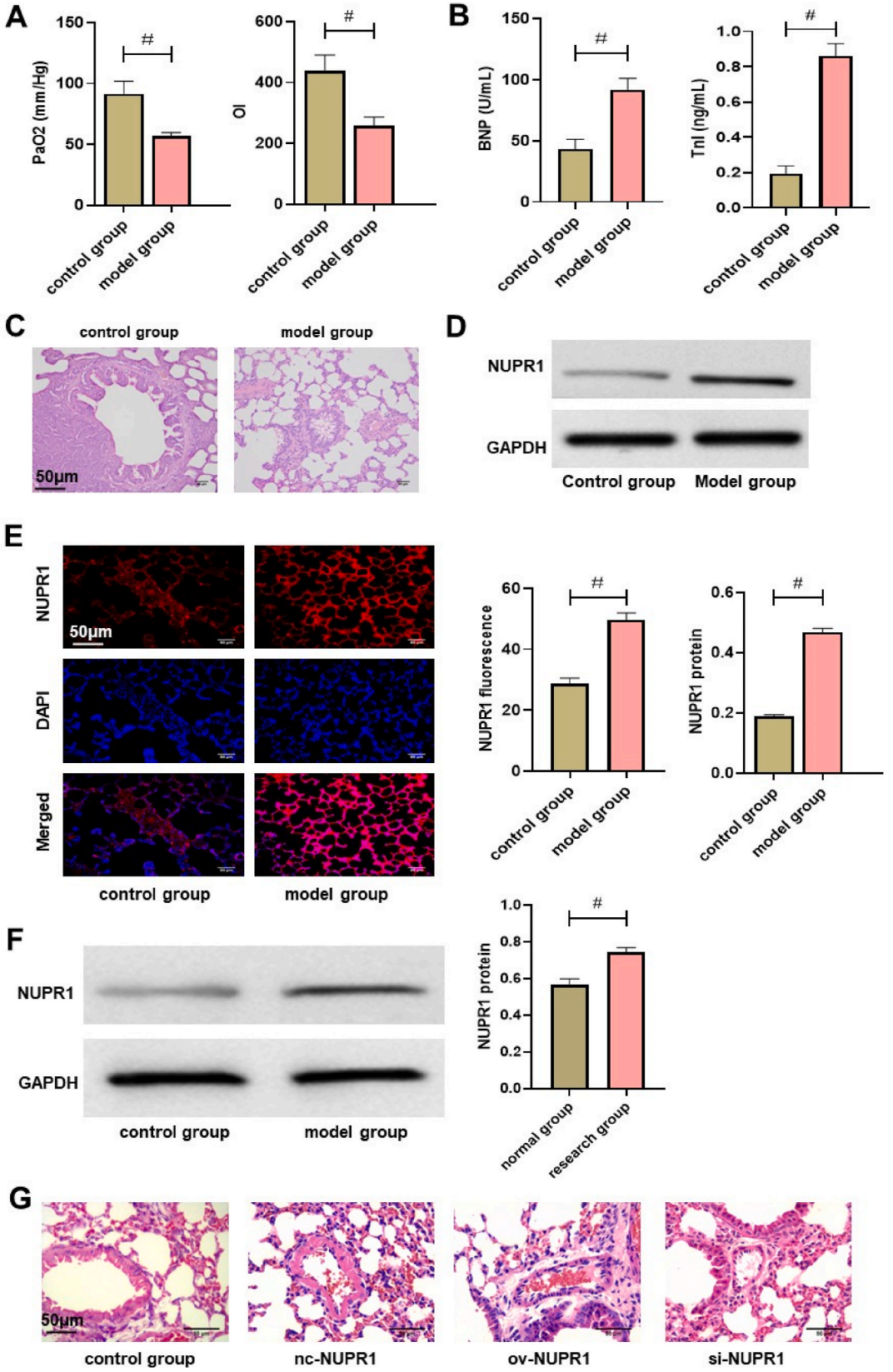

(caption on next page)

Fig. 1. Expression of NUPR1 in PE rats. A) Comparison of PaO2 and OI between control and model groups. (B) Comparison of BNP and TnI between control and model groups. (C) HE staining of lung tissue showing structural differences between control and model groups. (D) Comparison of NUPR1 protein expression between control and model groups. (E) Comparison of NUPR1 fluorescence intensity between control and model groups. (F) Comparison of NURP1 protein expression in research and normal group. (G) Effects of NUPR1 modulation on the histopathological condition of the lungs of PE rats. #P < 0.05.

paraformaldehyde and washed thrice with PBS. The membrane was then excised, mounted on a glass slide, and stained with 1 % crystal violet solution to facilitate the enumeration of transmembrane cells.

In the Scratch-Wound assay, the medium of confluent monolayer culture was gently scratched using the tip of a 200 μL pipette to create several wounds. Images were captured using a fluorescence microscope at 0 and 12 h post-scratching to monitor changes in scratch width. Cell migration was quantified using the formula: Migration percentage = [(initial scratch width - scratch width at 12 h)/ initial scratch width] × 100 %.

2.15. Protein localization

The cells were thoroughly washed with 1 × PBS, then fixed with 4 % PFA for 10–15 min. After fixation, the cells were permeabilized and blocked using 1 × PBS containing 2 % BSA and 0.3 % Triton X-100 for 30 min at room temperature. Primary antibodies, including NUPR1 (sc-33673, 1:50), CD44 (15675-1-AP, 1:50), α-SMA (AF1032, 1:200), vimentin (AF7013, 1:200), and Ki67 (AF0198, 1:100), were diluted in 1 × PBS with 2 % BSA and 0.3 % Triton X-100, added to the cells, and incubated overnight at 4 °C. The cells were then washed three times with 1 × PBS before applying secondary antibodies and Hoechst33342. This mixture was incubated at room temperature for 1 h, protected from light. Finally, the plate was securely sealed, and the results were observed and documented using a microscope.

2.16. Statistical methods

Statistical analyses were conducted using SPSS version 24.0 software, with a significance threshold set at P < 0.05. Results were presented as mean ± standard deviation (c ± s) exclusively. Intergroup comparisons were assessed using independent sample t-tests, while multi-group and multi-time-point comparisons were performed using repeated measures analysis of variance (ANOVA) followed by the LSD test for post-hoc analysis.

3. Results

3.1. Expression of NUPR1 in PE

To investigate the expression of NUPR1 in PE rats, we first measured the PaO2 and the OI in blood samples collected from the abdominal aorta with a blood gas analyzer. The results showed that both PaO2 and OI were significantly lower in the model group compared to the control group (Fig. 1A). We then utilized ELISA to measure levels of BNP and TnI. Our results showed that BNP and TnI were significantly elevated in the model group compared to the control group (Fig. 1B). Histological examination of lung tissue revealed notable differences between the groups. The control rats exhibited clear and intact lung tissue structures, whereas the model group showed signs of ruptured alveoli, exudate, interstitial edema, and infiltration of inflammatory cells (Fig. 1C). Subsequent analysis of NUPR1 protein expression in lung tissue showed a marked increase in the model group compared to the control group (Fig. 1D). Fluorescence staining further confirmed these findings, with the model group displaying significantly stronger NUPR1 expression (Fig. 1E). To further validate NUPR1 expression, we compared its levels in PASMCs between the research group and the normal group. The results demonstrated significantly higher NUPR1 protein expression in the research group compared to the control group (P < 0.05, Fig. 1F), indicating abnormal NUPR1 expression in PE. Following the intervention in PE rats using lentiviral vectors for aberrant NUPR1 expression, notable pathological changes were observed in the lung tissues across all experimental groups (nc-NUPR1, ov-NUPR1, and si-NUPR1) compared to the control group. However, significant differences were observed among the intervention groups. The si-NUPR1 group, which had reduced NUPR1 expression, displayed a marked improvement in lung tissue structure, with fewer instances of alveolar rupture and reduced interstitial edema. In contrast, the ov-NUPR1 group, which had increased NUPR1 expression, exhibited exacerbated pathological features, including edema and pronounced inflammatory infiltration, compared to the nc-NUPR1 group. These findings indicate that NUPR1 knockdown may protect against lung tissue damage in PE, while its overexpression may aggravate the pathological and inflammatory responses (Fig. 1G).

3.2. Effect of NUPR1 on the phenotypic transformation of PASMCs under normoxic conditions

To understand the role of NUPR1 in the phenotypic transformation of PASMCs under normoxic conditions, we cultured PASMCs under normoxic conditions, and NUPR1 protein expression was assessed at various time points. The results showed no significant changes in NUPR1 expression under these conditions indicating that NUPR1 does not exhibit any abnormal expression under normal conditions (Fig. 2A). Next, PASMCs were transfected with vectors to modulate NUPR1 expression. In the ov-NUPR1 group, NUPR1 levels were significantly higher compared to the nc-NUPR1 and si-NUPR1 groups, while the si-NUPR1 group showed lower NUPR1

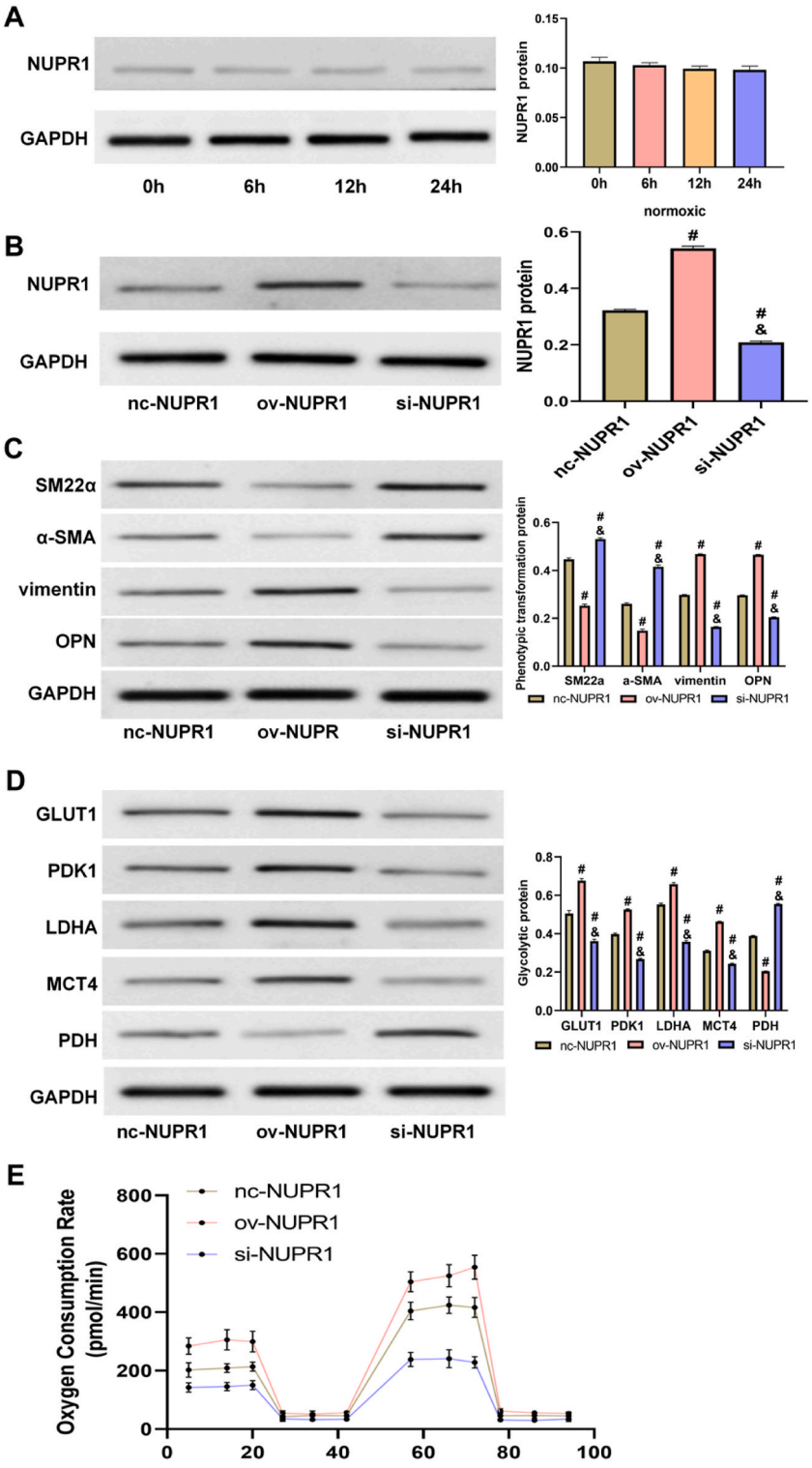

Fig. 2. Effect of NUPR1 on the phenotypic transformation of PASMCs under normoxic conditions. (A) NUPR1 expression in PASMCs under normoxic conditions at different time points. (B) NUPR1 expression in PASMCs following transfection with vectors to induce aberrant expression: ov-NUPR1 (overexpression), nc-NUPR1 (normal control), and si-NUPR1 (silencing). (C) Expression levels of phenotypic switching proteins: SM22α, α-SMA, Vimentin, and OPN. (D) Expression levels of glycolytic proteins: GLUT1, PDK1, LDHA, MCT4, and PDH. (E) The Seahorse assay was used to examine the impact of NUPR1 on oxygen consumption rates in PASMCs. *vs* nc-NUPR1 #P < 0.05, *vs* ov-NUPR1 &P < 0.05.

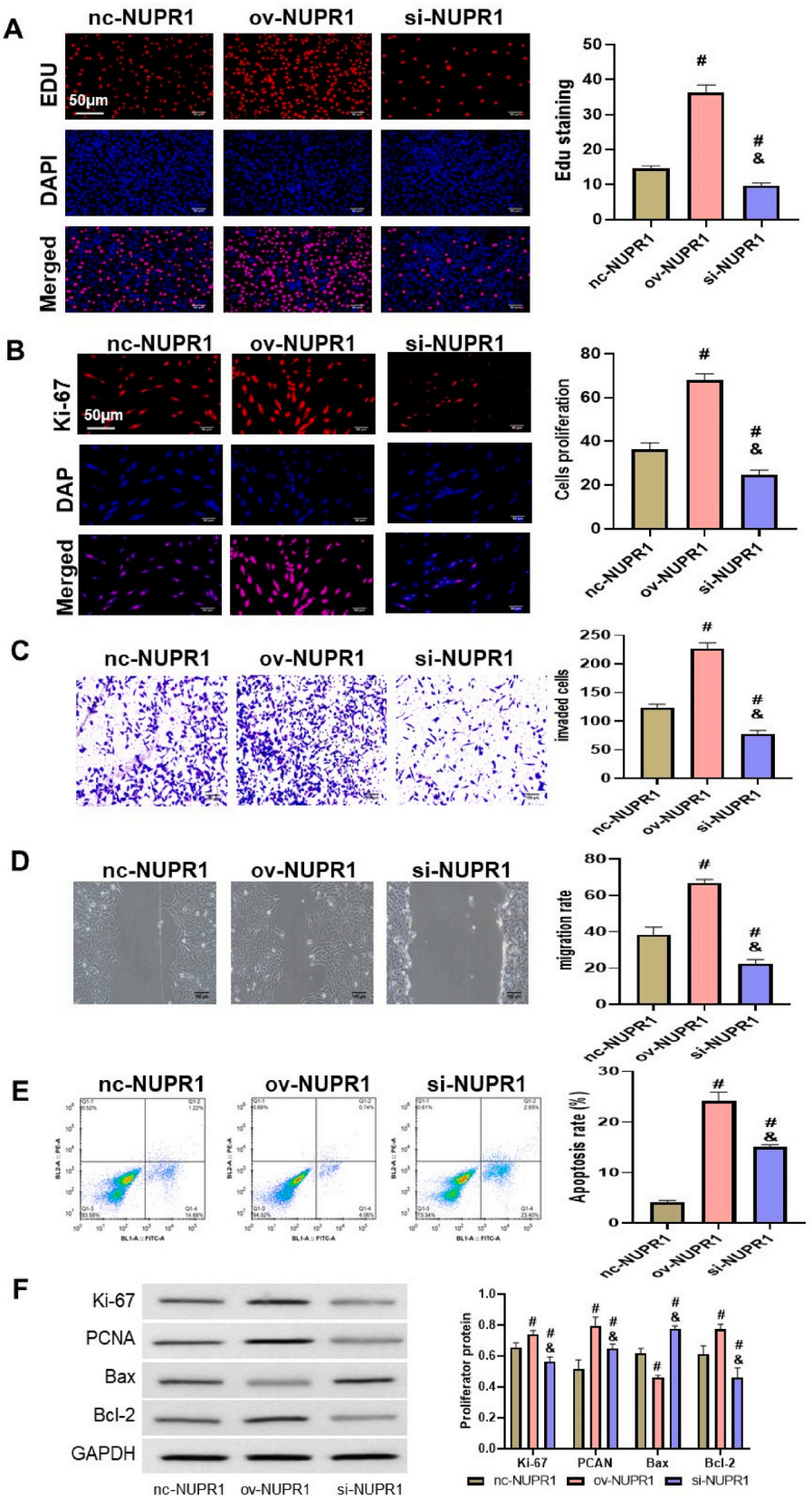

(caption on next page)

Fig. 3. Effect of NUPR1 on the activity of PASMCs under normoxic condition. (A) Comparison of cell proliferation rates using EdU incorporation assay. (B) Comparison of Ki-67 proliferation marker as an indicator of cell proliferation. (C) Comparison of cell invasion ability. (D) Comparison of cell migration ability. (E) Comparison of apoptosis rates. (F) Comparison of cell proliferation protein expression. *vs* nc-NUPR1 #P < 0.05, *vs* ov-NUPR1 &P < 0.05.

expression than the nc-NUPR1 group, confirming successful transfection (Fig. 2B). We then analyzed protein markers of secretion and phenotypic transformation to examine the effects of altered NUPR1 expression. Protein analysis revealed changes in markers of secretion and phenotypic transformation. Specifically, SM22α and α-SMA protein levels decreased in the ov-NUPR1 group, whereas Vimentin and OPN levels increased. Conversely, in the si-NUPR1 group, SM22α and α-SMA levels were elevated, and Vimentin and OPN levels were reduced (Fig. 2C). Additionally, we assessed glycolytic protein levels to investigate the impact of NUPR1 on glycolytic metabolism in PASMCs. Glycolytic protein levels were assessed. In the ov-NUPR1 group, the levels of GLUT1, PDK1, LDHA, and MCT4 were elevated, while PDH levels were decreased. The opposite pattern was observed in the si-NUPR1 group, where GLUT1, PDK1, LDHA, and MCT4 levels were reduced, and PDH levels were increased (Fig. 2D). Glycolysis levels were measured using the Seahorse assay, which showed a significant increase ($P < 0.05$) in both mitochondrial basal and maximal respiration following treatment with ov-NUPR1. In contrast, the si-NUPR1 group displayed a marked decrease ($P < 0.05$) in these glycolytic metrics (Fig. 2E). These results indicate that NUPR1 plays a crucial role in modulating the phenotypic transformation and glycolytic metabolism of PASMCs under normoxic conditions.

3.3. Effect of NUPR1 on the activity of PASMCs under normoxic condition

We investigated how NUPR1 influences the activity of PASMCs under normoxic conditions. First, we assessed the proliferation rate to determine the impact of NUPR1 on cell growth. We performed both Ki67 staining and EdU incorporation assays to measure cell proliferation. The results showed that the ov-NUPR1 group had a significantly higher proliferation rate compared to the nc-NUPR1 group. This was evidenced by increased Ki67 fluorescence intensity and higher EdU incorporation in the ov-NUPR1 group. Conversely, the si-NUPR1 group exhibited a significantly lower proliferation rate, with reduced Ki67 fluorescence intensity and lower EdU incorporation compared to the nc-NUPR1 group (Fig. 3A–B). Next, we evaluated the invasion and migration abilities of PASMCs to understand how NUPR1 affects cell motility. The invasion and migration abilities of the ov-NUPR1 group were significantly higher than those of the nc-NUPR1 group (Fig. 3C–D). In contrast, the si-NUPR1 group showed significantly reduced invasion and migration abilities compared to the nc-NUPR1 group (Fig. 3C–D). Flow cytometry revealed a significantly reduced apoptosis rate in the ov-NUPR1 group, while the si-NUPR1 group exhibited a higher apoptosis rate compared to the nc-NUPR1 group (Fig. 3E). Additionally, the ov-NUPR1 group showed elevated levels of Ki-67, PCNA, and the anti-apoptotic protein Bcl-2, with a corresponding decrease in the pro-apoptotic protein Bax ($P > 0.05$). In contrast, the si-NUPR1 group demonstrated the opposite pattern, with reduced Ki-67, PCNA, and Bcl-2 levels, and increased Bax expression ($P < 0.05$, Fig. 3F).

3.4. Effect of NUPR1 on the phenotypic transformation of PASMCs under hypoxia

We cultured PASMCs under hypoxic conditions and assessed the expression of NUPR1. Remarkably, NUPR1 protein expression exhibited a gradual increase with the duration of hypoxia and reached the highest value at 24 h (Fig. 4A). We then transfected NUPR1 expression vectors into PASMCs under hypoxia and found that NUPR1 expression was increased in the ov-NUPR1 group, but decreased in the si-NUPR1 group, confirming successful transfection (Fig. 4B). Similarly, in hypoxic cells, the expression of phenotypic transformation proteins such as SM22α and α-SMA was considerably reduced in the ov-NUPR1 group, while vimentin and OPN expression increased (Fig. 4C). These effects were reversed in the si-NUPR1 group, indicating a role for NUPR1 in regulating the phenotypic transformation of PASMCs under hypoxia. As glycolysis is related to cellular adaptation to hypoxia, we next investigated the expression of glycolytic proteins under similar conditions. We observed increased expression of GLUT1, PDK1, LDHA, and MCT4 in the ov-NUPR1 group, accompanied by reduced levels of PDH. Conversely, the expression of these proteins was reversed in the si-NUPR1 group (Fig. 4D). Similarly, the Seahorse assay confirmed a reduced glycolytic capacity in the si-NUPR1 group and an elevated capacity in the ov-NUPR1 group ($P < 0.05$, Fig. 4E). Overall, these findings highlight the critical role of NUPR1 in regulating the phenotypic transformation and glycolytic metabolism of PASMCs under hypoxic conditions.

3.5. Influence of NUPR1 on PASMCs activity under hypoxia

To comprehensively understand the influence of NUPR1 on PASMCs activity under hypoxic conditions, we conducted a series of experiments. First, we assessed cell proliferation using EdU incorporation assays to determine the impact of NUPR1 on PASMCs growth under hypoxia. The results showed a significant increase in the proliferation rate of the ov-NUPR1 group, while the si-NUPR1 group exhibited decreased proliferation compared to the nc-NUPR1 group (Fig. 5A). Next, we evaluated cell proliferation using Ki67 expression as an additional marker. Consistently, Ki67 staining indicated higher proliferation in the ov-NUPR1 group compared to the nc-NUPR1 and si-NUPR1 groups, while proliferation was lower in the si-NUPR1 group compared to the nc-NUPR1 group demonstrating enhanced sensitivity to hypoxia-induced cells proliferation (Fig. 5B). In Transwell and scratch-wound assays, which assess cell invasion and migration abilities, respectively, the ov-NUPR1 group demonstrated the highest invasion and migration capabilities among the three groups, while the si-NUPR1 group exhibited the lowest (Fig. 5C–D). Similarly, the apoptosis rate in the ov-NUPR1

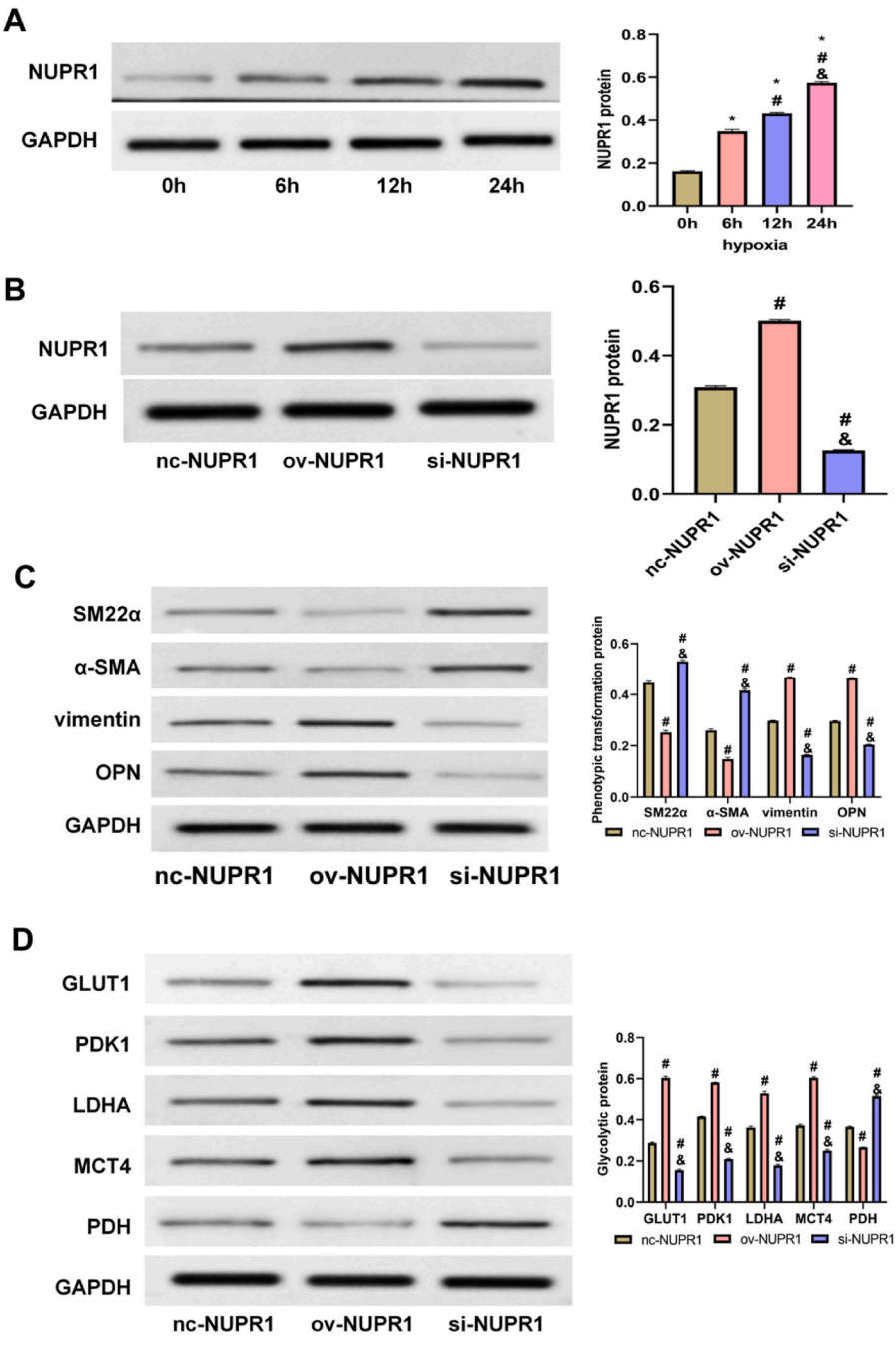

(caption on next page)

Fig. 4. Effect of NUPR1 on the phenotypic transformation of PASMCs under hypoxia. (A) Expression of NUPR1 under hypoxia at different time points, vs 0h *P < 0.05, vs 6h #P < 0.05, vs 12h vs 24h &P < 0.05. (B) Expression of NUPR1 after transfection of aberrant expression vectors, (C) Expression of phenotypic transformation proteins. (D) Expression of glycolytic proteins. (E) The Seahorse assay was used to examine the impact of NUPR1 on oxygen consumption rates in PASMC. *vs* nc-NUPR1 #P < 0.05, *vs* ov-NUPR1 &P < 0.05.

group was significantly reduced, while the si-NUPR1 group exhibited a higher apoptosis rate compared to the nc-NUPR1 group (Fig. 5E). Additionally, the ov-NUPR1 group showed elevated levels of proliferative proteins, including Ki-67, PCNA, and the anti-apoptotic protein Bcl-2, alongside a decrease in Bax expression (P > 0.05). In contrast, the si-NUPR1 group demonstrated the opposite pattern, with reduced levels of Ki-67, PCNA, and Bcl-2, and an increase in Bax expression (P < 0.05, Fig. 5F). Overall, NUPR1 plays a crucial role in regulating PASMCs activity under hypoxic conditions, impacting proliferation, invasion, and migration capabilities.

3.6. Localization of NUPR1 and phenotypic proteins in PASMsC

We next examined the subcellular localization of NUPR1 and phenotypic proteins in PASMCs. Fluorescent staining revealed that NUPR1 is predominantly localized in the nucleus of PASMCs. Furthermore, SM22α was observed on the cell membrane, α-SMA was concentrated within filamentous structures at the cell periphery, and both vimentin and OPN were found to be localized in the cytoplasm (Fig. 6). Overall, this indicates that NUPR1 and these phenotypic proteins have distinct and specific roles in regulating the structure and function of PASMCs.

4. Discussion

PE involves intricate changes in vascular structure and function, pivotal for developing targeted therapies [24]. Physiologically, the pulmonary artery intima provides a vast and unobstructed surface for blood flow in the pulmonary circulation, facilitating gas exchange and maintaining a low perfusion pressure [25]. The tunica media of the pulmonary artery primarily comprises PASMCs, serving as the foundation for PE initiation [26]. Research indicates that PASMCs undergo abnormal proliferation under external stimuli such as hypoxia and inflammation, leading to pulmonary vascular thickening, lumen stenosis, and migration towards the tunica intima. These changes result in structural and functional abnormalities in pulmonary vessels and a subsequent irreversible increase in pulmonary vascular perfusion pressure, ultimately culminating in PE [23]. Hence, targeting the aberrant biological behavior of PASMCs may represent a novel approach for PE treatment.

NUPR1 is a member of AT-hook-containing chromosomal DNA-binding proteins. Akin to other structural chromatin-binding proteins, it plays a role in various DNA-related events, including gene transcription, DNA repair, and chromosome recombination [27,28]. Additionally, NUPR1 serves as a multifunctional stress-inducing protein, and responds to environmental pressures such as oxidative damage and unfolded protein reactions [29]. In this study, we investigated the impact of NUPR1 on PASMCs, laying the groundwork for potential future molecular targeted therapies involving NUPR1.

Given the current lack of understanding regarding specific role of NUPR1 in PE, we initially assessed its expression. Following PE induction via autologous pulmonary emboli infusion into the jugular vein, the model group exhibited decreased PaO2 and OI levels, alongside increased BNP and TnI levels. Additionally, pulmonary tissue staining revealed alveolar rupture, exudate, interstitial edema, and extensive inflammatory cell infiltration, consistent with pathological changes observed in PE [30]. Further analysis of NUPR1 expression revealed higher levels in the model group compared to the control group, indicating abnormal elevation of NUPR1 in PE. Consistent with our findings, prior studies have reported similarly elevated NUPR1 levels in conditions such as oral and bladder cancer [31–33]).

As previously discussed, the aberrant behavior of PASMCs forms the crux of PE progression, so it is necessary to further analyze the influence of NUPR1 in PASMCs. Initial observations on PASMCs isolated from SD rats revealed no significant change in NUPR1 expression under normoxic conditions, indicating its normal expression levels in physiological settings. However, manipulating NUPR1 expression in PASMCs revealed noteworthy outcomes i.e. NUPR1 overexpression suppressed the expression of contractile phenotype markers α-SMA and SM22α, while inducing the expression of synthetic phenotype markers Vimentin and OPN. Conversely, silencing NUPR1 expression yielded opposite effects. These alterations signify reduced cell proliferation and extracellular matrix synthesis, accelerating PASMCs phenotypic transformation and pulmonary vascular remodeling [34]. This aligns with our findings in PE rats, highlighting NUPR1's role in stimulating PASMCs phenotypic transformation and PE progression.

Furthermore, to substantiate our findings, we constructed pathological PASMCs models under both hypoxic and normoxic conditions as shown previously [35]. Here, NUPR1 expression gradually increased with prolonged hypoxia exposure, suggesting a link between cellular hypoxia and heightened NUPR1 expression. Notably, role of NUPR1 as a key transcription factor in mitigating oxidative damage and anti-ferroptosis underlines its response to stress injury during hypoxia [36]. This dysregulation, exacerbated by interference with NUPR1 expression, mirrored observations in normoxic PASMCs, and reinforces the impact of NUPR1 on phenotypic transformation of PASMCs under pathological conditions. Moreover, elevated NUPR1 expression significantly enhanced PASMCs proliferation, invasion, and migration, corroborating its role in inducing abnormal PASMCs proliferation through phenotypic transformation, ultimately contributing to PE development. This finding is consistent with prior studies linking NUPR1 to increased proliferation and metastasis at least in cancers [18,31,37].

Glycolysis is a vital process for cellular energy production, where glucose is broken down into pyruvate, generating ATP [38]. This

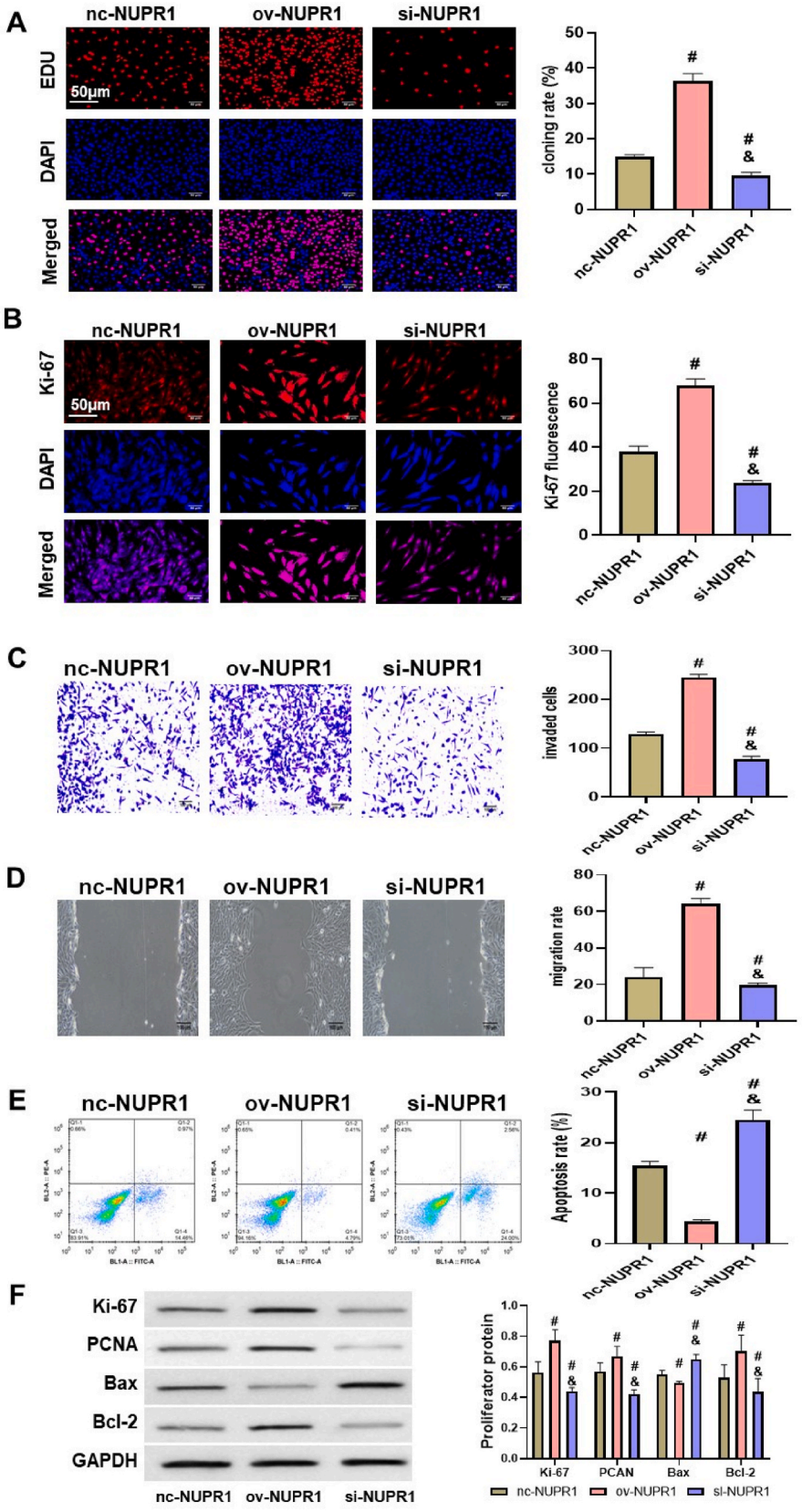

(caption on next page)

Fig. 5. Influence of NUPR1 on PASMCs activity under hypoxia. A) Comparison of cell activity, B) Comparison of Ki-67 fluorescence intensity, C) Comparison of cell invasion ability, D) Comparison of cell migration ability. (E) Comparison of apoptosis rates. (F) Comparison of cell proliferation protein expression. *vs* nc-NUPR1 #P < 0.05, *vs* ov-NUPR1 &P < 0.05.

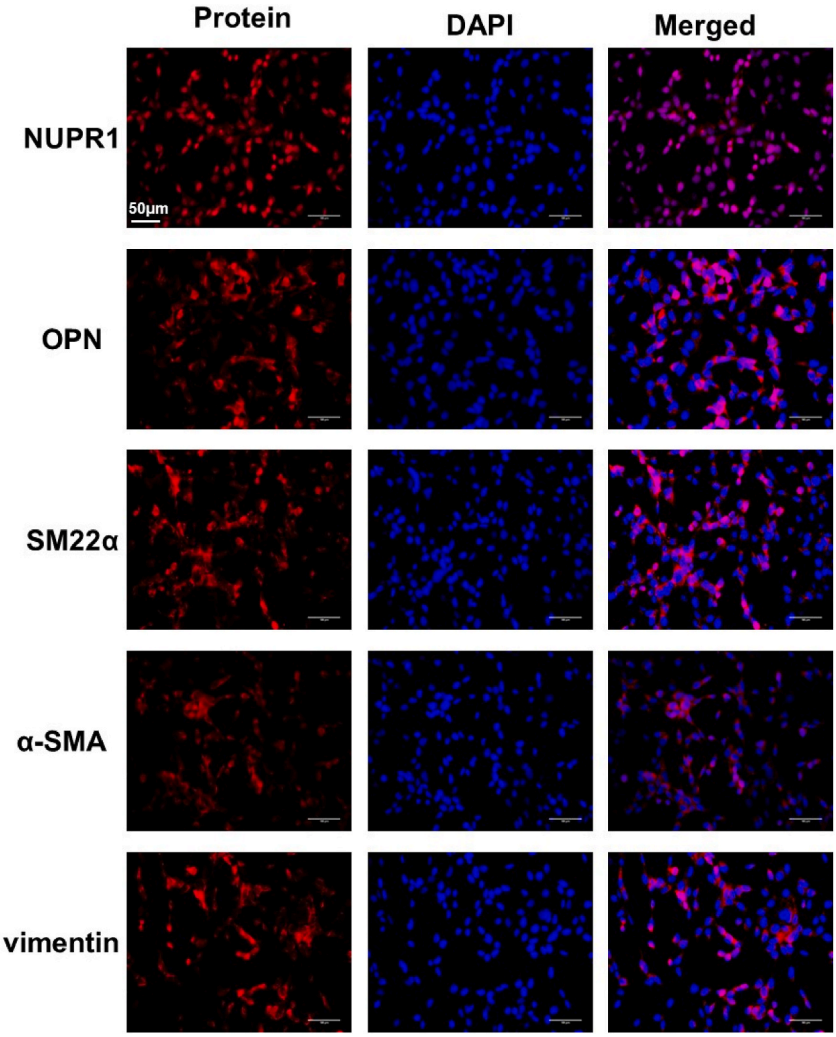

Fig. 6. Subcellular localization of NUPR1, OPN, SM22α, α-SMA, and vimentin in PASMCs. Fluorescent staining shows NUPR1 primarily in the nucleus, SM22α on the cell membrane, α-SMA in filamentous structures at the cell periphery, and vimentin and OPN within the cytoplasm, highlighting their distinct roles in PASMCs.

pathway is crucial for understanding PASMCs phenotypic transition, as increased glycolysis in these cells can lead to extracellular acidification and activation of acid-sensing ion channels [39]. Hypoxia has been shown to enhance glycolysis in PASMCs by promoting protein misfolding and activating PERK signaling, which increases cell viability and proliferation [40]. NUPR1, known for its regulatory role in glycolysis [41] may similarly influence PASMCs by controlling the expression of glycolysis-related proteins. Glucose transport into cells is a crucial step in glucose metabolism, regulated by a family of glucose transporter proteins, including GLUT1-GLUT14 [42]. GLUT1, the primary glucose transporter in PASMCs, facilitates glucose uptake, which is then converted to pyruvate [43,44]). Pyruvate can either be converted to lactate or enter mitochondria for further oxidation, with PDK1 inhibiting this process by phosphorylating PDH [33,45]. Elevated lactate levels can inhibit glycolysis, but this effect is mitigated by lactate secretion via MCT4 [46]. Our study found that increased NUPR1 expression promotes glycolysis in PASMCs, suggesting that NUPR1 drives the phenotypic transformation of these cells by regulating glycolytic pathways.

In our study, we observed the nuclear localization of NUPR1 within PASMCs, confirming its nuclear origin. It is well established that the proper functioning of mature proteins depends on their presence in specific subcellular locations [47]. While most proteins are synthesized in the cytoplasm or rough endoplasmic reticulum before being transported to specific subcellular locations for proper function [48], our study suggests that NUPR1, as a nuclear protein, plays a crucial role in PASMCs function. It supports DNA structure,

facilitates chromosomal assembly, and influences the localization of SM22α, vimentin, and OPN. Additionally, the activation of α-SMA near the cell periphery enhances fibril synthesis, contributing to emboli formation. These insights highlight the critical role of NUPR1 in PASMCs phenotypic transition.

While our study provides valuable insights, it has several limitations. We did not investigate the mechanisms by which NUPR1 exerts its effects, particularly its potential role in regulating autophagy, as suggested by previous research [49]. Further investigation into the pathological mechanisms, toxicity, and side effects of NUPR1 modulation in animal models is necessary. Additionally, incorporating large number of clinical cases to confirm the exact role of NUPR1 in PE will offer a more reliable foundation for its clinical application. Future research should explore the broader implications of NUPR1's role in PE, particularly focusing on the development of targeted therapeutic interventions. The potential for molecular therapies that suppress NUPR1 offers a promising avenue for innovative PE treatments. Moreover, examining NUPR1's interactions with other molecular pathways could reveal new mechanisms driving PE progression and identify additional therapeutic targets.

Funding

This study was not supported by any external funding.

Ethics statement

All the experimental procedures involving animals were conducted in accordance with ARRIVE guidelines and approved by the Animal Ethics Committee of Zibo Central Hospital (No. 2023WSA010008). The study involving human subjects complied with the Declaration of Helsinki and was approved by the ethical committee of the Zibo Central Hospital (No. 20230108), and all participants provided written informed consent.

Consent for publication

Not applicable.

Data availability statement

The original data presented in the study are included in the article. Further inquiries can be directed to the corresponding authors.

CRediT authorship contribution statement

Shu Wang: Validation, Software, Resources, Methodology. **Aizhen Xu:** Software, Methodology, Formal analysis, Data curation, Conceptualization. **Maoqing Chen:** Writing – review & editing, Software, Resources. **Yue Wu:** Writing – original draft, Supervision, Resources, Project administration, Funding acquisition, Formal analysis.

Declaration of competing interest

The authors declare that they have no known competing financial interests or personal relationships that could have appeared to influence the work reported in this paper.

Acknowledgements

None.

Appendix A. Supplementary data

Supplementary data to this article can be found online at https://doi.org/10.1016/j.heliyon.2024.e38918.

References

[1] M. Turetz, A.T. Sideris, O.A. Friedman, N. Triphathi, J.M. Horowitz, Epidemiology, pathophysiology, and natural history of pulmonary embolism, Semin. Intervent. Radiol. 35 (2) (2018) 92–98, https://doi.org/10.1055/s-0038-1642036.
[2] G.S. Alotaibi, C. Wu, A. Senthilselvan, M.S. McMurtry, Secular trends in incidence and mortality of acute venous thromboembolism: the AB-VTE population-based study 129 (8) (2016) 879. e819–e879. e825.
[3] K.T. Horlander, D.M. Mannino, K.V. Leeper, Pulmonary embolism mortality in the United States, 1979-1998: an analysis using multiple-cause mortality data 163 (14) (2003) 1711–1717.
[4] E.O. Essien, P. Rali, S.C. Mathai, Pulmonary embolism, Med. Clin. 103 (3) (2019) 549–564, https://doi.org/10.1016/j.mcna.2018.12.013.

[5] L. Falsetti, E. Guerrieri, V. Zaccone, G. Viticchi, S. Santini, L. Giovenali, G. Moroncini, Cutting-edge techniques and drugs for the treatment of pulmonary embolism: current knowledge and future perspectives, J. Clin. Med. 13 (7) (2024), https://doi.org/10.3390/jcm13071952.

[6] F.H.J. Kaptein, L.J.M. Kroft, G. Hammerschlag, M.K. Ninaber, M.P. Bauer, M.V. Huisman, F.A. Klok, Pulmonary infarction in acute pulmonary embolism, Thromb. Res. 202 (2021) 162–169, https://doi.org/10.1016/j.thromres.2021.03.022.

[7] B. Rivera-Lebron, M. McDaniel, K. Ahrar, A. Alrifai, D.M. Dudzinski, C. Fanola, P. Consortium, Diagnosis, treatment and follow up of acute pulmonary embolism: consensus practice from the PERT consortium, Clin. Appl. Thromb. Hemost. 25 (2019), https://doi.org/10.1177/1076029619853037, 1076029619853037.

[8] P. Monteleone, R. Ahern, S. Banerjee, K.R. Desai, D. Kadian-Dodov, E. Webber, S.A. Parikh, Modern treatment of pulmonary embolism (USCDT vs MT): results from a real-world, big data analysis (REAL-PE), Journal of the Society for Cardiovascular Angiography & Interventions 3 (1) (2024) 101192, https://doi.org/10.1016/j.jscai.2023.101192.

[9] T. Trott, J. Bowman, Diagnosis and management of pulmonary embolism, Emerg. Med. Clin. 40 (3) (2022) 565–581, https://doi.org/10.1016/j.emc.2022.05.008.

[10] J.A. Kline, Diagnosis and exclusion of pulmonary embolism, Thromb. Res. 163 (2018) 207–220, https://doi.org/10.1016/j.thromres.2017.06.002.

[11] J. Liu, X. Song, F. Kuang, Q. Zhang, Y. Xie, R. Kang, D. Tang, NUPR1 is a critical repressor of ferroptosis, Nat. Commun. 12 (1) (2021) 647, https://doi.org/10.1038/s41467-021-20904-2.

[12] S. Liu, M. Costa, The role of NUPR1 in response to stress and cancer development, Toxicol. Appl. Pharmacol. 454 (2022) 116244, https://doi.org/10.1016/j.taap.2022.116244.

[13] S. Liu, M. Costa, The role of NUPR1 in response to stress and cancer development, Toxicol. Appl. Pharmacol. 454 (2022) 116244, https://doi.org/10.1016/j.taap.2022.116244.

[14] J. Averous, S. Lambert-Langlais, Y. Cherasse, V. Carraro, L. Parry, W. B'chir, B.R. Communications, Amino acid deprivation regulates the stress-inducible gene p8 via the GCN2/ATF4 pathway 413 (1) (2011) 24–29.

[15] A. Carracedo, M. Lorente, A. Egia, C. Blázquez, S. García, V. Giroux, González-Feria, L. J. C. c, The stress-regulated protein p8 mediates cannabinoid-induced apoptosis of tumor cells 9 (4) (2006) 301–312.

[16] Y.-F. Jiang, M.I. Vaccaro, F. Fiedler, E.L. Calvo, J.L.J.B. Iovanna, b. r. communications, Lipopolysaccharides induce p8 mRNA expression in vivo and in vitro 260 (3) (1999) 686–690.

[17] P. Santofimia-Castaño, N. Fraunhoffer, X. Liu, I.F. Bessone, M.P. di Magliano, S. Audebert, J. Iovanna, Targeting NUPR1-dependent stress granules formation to induce synthetic lethality in Kras(G12D)-driven tumors, EMBO Mol. Med. 16 (3) (2024) 475–505, https://doi.org/10.1038/s44321-024-00032-2.

[18] P. Santofimia-Castano, Y. Xia, L. Peng, A. Velazquez-Campoy, O. Abian, W. Lan, J. Iovanna, Targeting the stress-induced protein NUPR1 to treat pancreatic adenocarcinoma, Cells 8 (11) (2019), https://doi.org/10.3390/cells8111453.

[19] Y.J. Kim, S.-E. Hong, S.-K. Jang, K.S. Park, C.-H. Kim, I.-C. Park, H.-O. Jin, Knockdown of NUPR1 enhances the sensitivity of non-small-cell lung cancer cells to metformin by AKT inhibition, Anticancer Res. 42 (7) (2022) 3475, https://doi.org/10.21873/anticanres.15834.

[20] H. Wang, D. Liu, H. Chen, Y. Jiao, H. Zhao, Z. Li, Y. Lan, Nupr1 negatively regulates endothelial to hematopoietic transition in the aorta-gonad-mesonephros region, Adv. Sci. 10 (6) (2023) e2203813, https://doi.org/10.1002/advs.202203813.

[21] J. Zhou, D. Guo, Z.Z. Xu, J.S. Liao, X.T. Li, K. Duan, W.B. Xie, Nupr1-mediated vascular smooth muscle cell phenotype transformation involved in methamphetamine induces pulmonary hypertension, Cell Biol. Toxicol. 40 (1) (2024) 13, https://doi.org/10.1007/s10565-024-09849-6.

[22] R. Zhou, J. Liao, D. Cai, Q. Tian, E. Huang, T. Lu, W.B. Xie, Nupr1 mediates renal fibrosis via activating fibroblast and promoting epithelial-mesenchymal transition, Faseb. J. 35 (3) (2021) e21381, https://doi.org/10.1096/fj.202000926RR.

[23] Y. Li, J. Shao, J. Song, S. Yu, J. Wang, K. Sun, MiR-34a-3p suppresses pulmonary vascular proliferation in acute pulmonary embolism rat by targeting DUSP1, Biosci. Rep. 42 (1) (2022), https://doi.org/10.1042/BSR20210116.

[24] P.M. Rali, G.J. Criner, Submassive pulmonary embolism, Am. J. Respir. Crit. Care Med. 198 (5) (2018) 588–598, https://doi.org/10.1164/rccm.201711-2302CI.

[25] A. Machanahalli Balakrishna, V. Reddi, P.M. Belford, M. Alvarez, W.A. Jaber, D.X. Zhao, S. Vallabhajosyula, Intermediate-risk pulmonary embolism: a review of contemporary diagnosis, risk stratification and management, Medicina (Kaunas) 58 (9) (2022), https://doi.org/10.3390/medicina58091186.

[26] H. Chen, Q. Ma, J. Zhang, Y. Meng, L. Pan, H. Tian, miR-106b-5p modulates acute pulmonary embolism via NOR1 in pulmonary artery smooth muscle cells, Int. J. Mol. Med. 45 (5) (2020) 1525–1533, https://doi.org/10.3892/ijmm.2020.4532.

[27] D.W. Clark, A. Mitra, R.A. Fillmore, W.G. Jiang, R.S. Samant, O. Fodstad, L.A. Shevde, NUPR1 interacts with p53, transcriptionally regulates p21 and rescues breast epithelial cells from doxorubicin-induced genotoxic stress, Curr. Cancer Drug Targets 8 (5) (2008) 421–430, https://doi.org/10.2174/156800908785133196.

[28] S. Vasseur, G.V. Mallo, A. Garcia-Montero, E.M. Ortiz, F. Fiedler, E. Cánepa, J.L.J.B.J. Iovanna, Structural and functional characterization of the mouse p8 gene: promotion of transcription by the CAAT-enhancer binding protein α (C/EBPα) and C/EBPβ trans-acting factors involves a C/EBP cis-acting element and other regions of the promoter 343 (2) (1999) 377–383.

[29] T.A. Martin, A.X. Li, A.J. Sanders, L. Ye, K. Frewer, R. Hargest, W.G. Jiang, NUPR1 and its potential role in cancer and pathological conditions, Int. J. Oncol. 58 (5) (2021), https://doi.org/10.3892/ijo.2021.5201 (Review).

[30] J. Zagorski, J.A. Kline, Differential effect of mild and severe pulmonary embolism on the rat lung transcriptome, Respir. Res. 17 (1) (2016) 86, https://doi.org/10.1186/s12931-016-0405-9.

[31] T. Fan, X. Wang, S. Zhang, P. Deng, Y. Jiang, Y. Liang, Z. Zhang, NUPR1 promotes the proliferation and metastasis of oral squamous cell carcinoma cells by activating TFE3-dependent autophagy, Signal Transduct. Targeted Ther. 7 (1) (2022) 130, https://doi.org/10.1038/s41392-022-00939-7.

[32] S.M.A. Mansour, S.A. Ali, S. Nofal, S.H. Soror, Targeting NUPR1 for cancer treatment: a risky endeavor, Curr. Cancer Drug Targets 20 (10) (2020) 768–778, https://doi.org/10.2174/1568009620666200703152523.

[33] C. Zhang, Y. Sun, Y. Guo, J. Xu, H. Zhao, JMJD1C promotes smooth muscle cell proliferation by activating glycolysis in pulmonary arterial hypertension, Cell Death Dis. 9 (1) (2023) 98, https://doi.org/10.1038/s41420-023-01390-5.

[34] A. Yamamura, N. Ohara, K. Tsukamoto, Inhibition of excessive cell proliferation by calcilytics in idiopathic pulmonary arterial hypertension, PLoS One 10 (9) (2015) e0138384, https://doi.org/10.1371/journal.pone.0138384.

[35] L. Wang, H.L. Gan, Y. Liu, S. Gu, J. Li, L.J. Guo, C. Wang, The distinguishing cellular features of pulmonary artery smooth muscle cells from chronic thromboembolic pulmonary hypertension patients, Exp. Lung Res. 39 (8) (2013) 349–358, https://doi.org/10.3109/01902148.2013.822947.

[36] C. Huang, P. Santofimia-Castano, J. Iovanna, NUPR1: a critical regulator of the antioxidant system, Cancers 13 (15) (2021), https://doi.org/10.3390/cancers13153670.

[37] G. Augello, M.R. Emma, A. Azzolina, R. Puleio, L. Condorelli, A. Cusimano, M. Cervello, The NUPR1/p73 axis contributes to sorafenib resistance in hepatocellular carcinoma, Cancer Lett. 519 (2021) 250–262, https://doi.org/10.1016/j.canlet.2021.07.026.

[38] S.J. Kierans, C.T. Taylor, Regulation of glycolysis by the hypoxia-inducible factor (HIF): implications for cellular physiology, J. Physiol. 599 (1) (2021) 23–37, https://doi.org/10.1113/JP280572.

[39] M.N. Tuineau, L.M. Herbert, S.M. Garcia, T.C. Resta, N.L. Jernigan, Enhanced glycolysis causes extracellular acidification and activates acid-sensing ion channel 1a in hypoxic pulmonary hypertension, Am. J. Physiol. Lung Cell Mol. Physiol. (2024), https://doi.org/10.1152/ajplung.00083.2024.

[40] T. Shimizu, Y. Higashijima, Y. Kanki, R. Nakaki, T. Kawamura, Y. Urade, Y. Wada, PERK inhibition attenuates vascular remodeling in pulmonary arterial hypertension caused by BMPR2 mutation, Sci. Signal. 14 (667) (2021), https://doi.org/10.1126/scisignal.abb3616.

[41] K. Matsunaga, K. Fujisawa, T. Takami, G. Burganova, N. Sasai, T. Matsumoto, I. Sakaida, NUPR1 acts as a pro-survival factor in human bone marrow-derived mesenchymal stem cells and is induced by the hypoxia mimetic reagent deferoxamine, J. Clin. Biochem. Nutr. 64 (3) (2019) 209–216, https://doi.org/10.3164/jcbn.18-112.

[42] A. Chadt, H. Al-Hasani, Glucose transporters in adipose tissue, liver, and skeletal muscle in metabolic health and disease, Pflueg. Arch. Eur. J. Physiol. 472 (9) (2020) 1273–1298, https://doi.org/10.1007/s00424-020-02417-x.

[43] Y. Chen, J. Joo, J.M.-T. Chu, R.C.-C. Chang, G.T.-C. Wong, Downregulation of the glucose transporter GLUT 1 in the cerebral microvasculature contributes to postoperative neurocognitive disorders in aged mice, J. Neuroinflammation 20 (1) (2023) 237, https://doi.org/10.1186/s12974-023-02905-8.
[44] D. Li, N.Y. Shao, J.R. Moonen, Z. Zhao, M. Shi, S. Otsuki, M. Rabinovitch, ALDH1A3 coordinates metabolism with gene regulation in pulmonary arterial hypertension, Circulation 143 (21) (2021) 2074–2090, https://doi.org/10.1161/CIRCULATIONAHA.120.048845.
[45] L. Luo, L. Xiao, G. Lian, H. Wang, L. Xie, miR-125a-5p inhibits glycolysis by targeting hexokinase-II to improve pulmonary arterial hypertension, Aging (Albany NY) 12 (10) (2020) 9014–9030, https://doi.org/10.18632/aging.103163.
[46] J. Ryan, A. Dasgupta, J. Huston, K.H. Chen, S.L. Archer, Mitochondrial dynamics in pulmonary arterial hypertension, J. Mol. Med. (Berl.) 93 (3) (2015) 229–242, https://doi.org/10.1007/s00109-015-1263-5.
[47] T. Wang, N. Yang, C. Liang, H. Xu, Y. An, S. Xiao, L. Nie, Detecting protein-protein interaction based on protein fragment complementation assay, Curr. Protein Pept. Sci. 21 (6) (2020) 598–610, https://doi.org/10.2174/1389203721666200213102829.
[48] S. Das, M. Vera, V. Gandin, R.H. Singer, E. Tutucci, Intracellular mRNA transport and localized translation, Nat. Rev. Mol. Cell Biol. 22 (7) (2021) 483–504, https://doi.org/10.1038/s41580-021-00356-8.
[49] L. Tan, R.R. Yammani, Nupr1 regulates palmitate-induced apoptosis in human articular chondrocytes, Biosci. Rep. 39 (2) (2019), https://doi.org/10.1042/BSR20181473.
[50] S. Goruppi, R.D. Patten, T. Force, J.M.J.M. Kyriakis, c. biology, Helix-loop-helix protein p8, a transcriptional regulator required for cardiomyocyte hypertrophy and cardiac fibroblast matrix metalloprotease induction 27 (3) (2007) 993–1006.